SCIENCE CHINA
Mathematics

Progress of Projects Supported by NSFC
• ARTICLES •

May 2021 Vol. 64 No. 5: 887–902
https://doi.org/10.1007/s11425-020-1817-4

Analysis of the second-order BDF scheme with variable steps for the molecular beam epitaxial model without slope selection

Hong-Lin Liao[1], Xuehua Song[1], Tao Tang[2,3,*] & Tao Zhou[4]

[1]*Department of Mathematics, Nanjing University of Aeronautics and Astronautics, Nanjing* 211101*, China;*
[2]*Department of Mathematics and International Center for Mathematics, Southern University of Science and Technology, Shenzhen* 518055*, China;*
[3]*Division of Science and Technology, BNU-HKBU United International College, Zhuhai* 519087*, China;*
[4]*NCMIS & LSEC, Institute of Computational Mathematics and Scientific Engineering Computing, Academy of Mathematics and Systems Science, Chinese Academy of Sciences, Beijing* 100190*, China*

Email: liaohl@nuaa.edu.cn, 1249734428@qq.com, tangt@sustech.edu.cn, tzhou@lsec.cc.ac.cn

Received April 12, 2020; accepted December 8, 2020; published online February 8, 2021

Abstract In this work, we are concerned with the stability and convergence analysis of the second-order backward difference formula (BDF2) with variable steps for the molecular beam epitaxial model without slope selection. We first show that the variable-step BDF2 scheme is convex and uniquely solvable under a weak time-step constraint. Then we show that it preserves an energy dissipation law if the adjacent time-step ratios satisfy $r_k := \tau_k/\tau_{k-1} < 3.561$. Moreover, with a novel discrete orthogonal convolution kernels argument and some new estimates on the corresponding positive definite quadratic forms, the L^2 norm stability and rigorous error estimates are established, under the same step-ratio constraint that ensures the energy stability, i.e., $0 < r_k < 3.561$. This is known to be the best result in the literature. We finally adopt an adaptive time-stepping strategy to accelerate the computations of the steady state solution and confirm our theoretical findings by numerical examples.

Keywords molecular beam epitaxial growth, variable-step BDF2 scheme, discrete orthogonal convolution kernels, energy stability, convergence analysis

MSC(2020) 74A50, 65M06, 65M12, 35Q99

Citation: Liao H-L, Song X H, Tang T, et al. Analysis of the second-order BDF scheme with variable steps for the molecular beam epitaxial model without slope selection. Sci China Math, 2021, 64: 887–902, https://doi.org/10.1007/s11425-020-1817-4

1 Introduction

We consider the following molecular beam epitaxial (MBE) model without slope selection on a bounded domain $\Omega \subset \mathbb{R}^2$:

$$\Phi_t = -\varepsilon\Delta^2\Phi - \nabla\cdot\boldsymbol{f}(\nabla\Phi) \quad \text{for } \boldsymbol{x}\in\Omega \quad \text{and} \quad 0 < t \leqslant T \tag{1.1}$$

subjected to the initial data $\Phi(\boldsymbol{x}, 0) := \Phi_0(\boldsymbol{x})$, where the nonlinear force vector $\boldsymbol{f}(\boldsymbol{v}) := \frac{\boldsymbol{v}}{1+|\boldsymbol{v}|^2}$. The unknown function $\Phi = \Phi(\boldsymbol{x}, t)$, subjected to the periodic boundary conditions, is the scaled height

* Corresponding author

function of a thin film in a co-moving frame and $\varepsilon > 0$ is a constant that represents the width of the rounded corners on the otherwise faceted crystalline thin films.

The above epitaxial growth model admits variable applications in different fields, such as physics [1], biology [9] and chemistry [22], to name a few. The MBE model (1.1), in which the nonlinear second-order term models the Ehrlich-Schwoebel effect and the linear fourth-order term describes the surface diffusion, defines a gradient flow with respect to the $L^2(\Omega)$ inner product of the following free energy [10, 16]:

$$E[\Phi] = \int_\Omega \left[\frac{\varepsilon}{2}(\Delta\Phi)^2 - \frac{1}{2}\ln(1 + |\nabla\Phi|^2)\right] d\boldsymbol{x}. \tag{1.2}$$

The logarithmic term therein is bounded above by zero but unbounded below (and has no relative minima), which implies that no energetically favored values exist for $\nabla\Phi$. From the physical point of view, this means that there is no slope selection mechanism. Thus, it may result in the multi-scale behavior in a rough-smooth-rough pattern, especially at an early stage of epitaxial growth on rough surfaces. The well-posedness of the initial-boundary-value problem (1.1) was studied by Li and Liu [16] using the perturbation analysis. It is shown in [16, Theorem 3.3] that, if the initial data $\phi_0 \in H^m_{\mathrm{per}}(\Omega)$ for some integer $m \geqslant 2$, there exists a unique weak solution $\phi \in L^\infty(0, T; H^m(\Omega)) \cap L^2(0, T; H^{m+2}(\Omega))$ and $\partial_t\phi \in L^2(0, T; H^{m-2}(\Omega))$. As is well known, the MBE system (1.1) is also volume-conservative, i.e., $(\Phi(t), 1) = (\Phi_0, 1)$ for $t > 0$, and admits the following energy dissipation law:

$$\frac{d}{dt}E[\Phi] = -\|\Phi_t\|^2_{L^2(\Omega)} \leqslant 0, \quad 0 < t \leqslant T, \tag{1.3}$$

where $(\cdot, \cdot)$ denotes the inner product in $L^2(\Omega)$ and $\|\cdot\|_{L^2(\Omega)}$ is the associated norm. Also, by the Green's formula and the Cauchy-Schwarz inequality, one has the L^2 norm solution estimate

$$\|\Phi\|_{L^2(\Omega)} \leqslant \mathrm{e}^{t/(4\varepsilon)}\|\Phi_0\|_{L^2(\Omega)}, \quad 0 < t \leqslant T. \tag{1.4}$$

As analytic solutions are not in general available, numerical schemes for the above MBE model have been widely studied in recent years [3, 4, 6, 12, 14, 20, 21, 23, 24, 26]; thus include the stabilized semi-implicit scheme [24], Crank-Nicolson type schemes [21], convex splitting schemes [3, 23], the exponential time differencing scheme [14], the invariant energy quadratization (IEQ) method [12, 26] and the scalar auxiliary variable (SAV) approach [6]. The main focus of the above-mentioned works was the discrete energy stability, i.e., one constructs a numerical scheme that can inherit the energy dissipation law in the discrete levels. Always, the IEQ and SAV methods transform the original system into a new equivalent system with a quadratic energy functional preserving the corresponding modified energy dissipation law. The SAV approach usually leads to numerical schemes involving only the decoupled equations with constant coefficients.

It is noticed that in all the above-mentioned literature, the numerical analysis was performed for uniform time-steps. In this work, we aim at investigating a nonuniform version of a classic numerical scheme, i.e., the second-order BDF (BDF2) scheme with variable time-steps. To this end, we consider the nonuniform time grids $0 = t_0 \leqslant t_1 \leqslant \cdots \leqslant t_N = T$ with the time-step sizes $\tau_k := t_k - t_{k-1}$. We denote the maximal step size by $\tau := \max_{1\leqslant k\leqslant N} \tau_k$ and define the local time-step ratio as $r_k := \tau_k/\tau_{k-1}$ for $k \geqslant 2$. Given a grid function $v^n = v(t_n)$, we set $\triangledown_\tau v^n := v^n - v^{n-1}$ and $\partial_\tau v^n := \triangledown_\tau v^n/\tau_n$ for $k \geqslant 1$. The motivation for using a nonuniform grid is that one can possibly capture the multi-scale behaviors in the time domain.

However, the numerical analysis for BDF2 with nonuniform grids seems to be highly nontrivial (compared with the uniform-grid case). A few results can be found in the literature. For the linear diffusion case, the existing L^2 norm stability and error estimates can be found in [2, 5, 8, 15]. However, for the analysis therein, the time-step ratio constraint that guarantees the L^2 norm stability are always severer than the classical zero-stability condition $r_k < 1 + \sqrt{2}$ for the ODE problems [7, 13]. Moreover, some undesired factors such as $\exp(C_r\Gamma_n)$ appear in the estimates, where Γ_n can be unbounded as the time-steps vanish and C_r grows to infinity once the step-ratios approach the zero-stability limit $1 + \sqrt{2}$. The associate analysis for nonlinear problems such as the Cahn-Hilliard (CH) equations can be found in [5]. Again, the error estimates therein are presented under the time-step constraints $r_k < 1.53$ (worse than the classical zero-stability condition).

As an exception, in our previous work [18], we have presented a novel analysis for the nonuniform BDF2 scheme of the Allen-Cahn equation under the same condition $r_k < 1+\sqrt{2}$. In a very recent work [19], for the linear diffusion problem, the L^2 norm stability and convergence estimates are presented under a much improved zero-stability condition

$$0 < r_k < r_s := (3+\sqrt{17})/2 \approx 3.561, \quad 2 \leqslant k \leqslant N.$$

In particular, a novel discrete orthogonal convolution (DOC) kernels argument related to the nonuniform BDF2 scheme is proposed to perform the analysis in [19]. In the current work, we will study the nonlinear MBE model under the new zero-stability condition.

1.1 The variable-step BDF2 scheme

The well-known nonuniform BDF2 formula can be expressed as the following convolutional summation:

$$D_2 v^n = \sum_{k=1}^{n} b_{n-k}^{(n)} \nabla_\tau v^k, \quad n \geqslant 1, \tag{1.5}$$

where the discrete convolution kernels $b_{n-k}^{(n)}$ are defined by $b_0^{(1)} := 1/\tau_1$ for $n=1$, and for $n \geqslant 2$ one has

$$b_0^{(n)} := \frac{1+2r_n}{\tau_n(1+r_n)}, \quad b_1^{(n)} := -\frac{r_n^2}{\tau_n(1+r_n)} \quad \text{and} \quad b_j^{(n)} := 0 \quad \text{for } j \geqslant 2. \tag{1.6}$$

Without loss of generality, we can include the first-order BDF (BDF1) formula in (1.5) by putting $r_1 \equiv 0$, and use it to compute the first-level solution for initialization.

To present the fully discrete scheme, for the physical domain $\Omega = (0, L)^2$, we use a uniform grid with grid lengths $h_x = h_y = h := L/M$ (with M being an integer) to yield the discrete domains

$$\Omega_h := \{\boldsymbol{x}_h = (ih, jh) \mid 1 \leqslant i, j \leqslant M\} \quad \text{and} \quad \bar{\Omega}_h := \{x_h = (ih, jh) \mid 0 \leqslant i, j \leqslant M\}.$$

For the function $w_h = w(\boldsymbol{x}_h)$, let

$$\Delta_x w_{ij} := (w_{i+1,j} - w_{i-1,j})/(2h) \quad \text{and} \quad \delta_x^2 w_{ij} = (w_{i+1,j} - 2w_{ij} + w_{i-1,j})/h^2.$$

The operators $\Delta_y w_{ij}$ and $\delta_y^2 w_{ij}$ can be defined similarly. Moreover, the discrete gradient vector and the discrete Laplacian can also be defined accordingly:

$$\nabla_h w_{ij} := (\Delta_x w_{ij}, \Delta_y w_{ij})^{\mathrm{T}}, \quad \Delta_h w_{ij} := (\delta_x^2 + \delta_y^2) w_{ij}.$$

One can further define the discrete divergence as $\nabla_h \cdot \boldsymbol{u}_{ij} := \Delta_x v_{ij} + \Delta_y w_{ij}$ for the vector $\boldsymbol{u}_h = (v_h, w_h)^{\mathrm{T}}$. We also denote the space of L-periodic grid functions by $\mathbb{V}_h := \{v_h \mid v_h \text{ is } L\text{-periodic for } \boldsymbol{x}_h \in \bar{\Omega}_h\}$.

We are now ready to present the fully implicit variable-step BDF2 scheme for the MBE equation (1.1): find the numerical solution $\phi_h^n \in \mathbb{V}_h$ such that $\phi_h^0 := \Phi_0(\boldsymbol{x}_h)$ and

$$D_2 \phi_h^n + \varepsilon \Delta_h^2 \phi_h^n + \nabla_h \cdot \boldsymbol{f}(\nabla_h \phi_h^n) = 0 \quad \text{for } \boldsymbol{x}_h \in \Omega_h \quad \text{and} \quad 1 \leqslant n \leqslant N. \tag{1.7}$$

1.2 Summary of the main contributions

As mentioned, we shall pursuit the further study of the analysis technique in [19] for the nonlinear MBE model. In [19], the discrete orthogonal convolution (DOC) kernels are proposed for analyzing the linear diffusion problems. The DOC kernels are defined as follows:

$$\theta_0^{(n)} := \frac{1}{b_0^{(n)}} \quad \text{and} \quad \theta_{n-k}^{(n)} := -\frac{1}{b_0^{(k)}} \sum_{j=k+1}^{n} \theta_{n-j}^{(n)} b_{j-k}^{(j)} \quad \text{for } 1 \leqslant k \leqslant n-1. \tag{1.8}$$

It is easy to verify that the following discrete orthogonal identity holds:

$$\sum_{j=k}^{n} \theta_{n-j}^{(n)} b_{j-k}^{(j)} \equiv \delta_{nk} \quad \text{for } 1 \leqslant k \leqslant n, \tag{1.9}$$

where δ_{nk} is the Kronecker delta symbol.

The main motivation for introducing the DOC kernels lies in the following equality:

$$\sum_{j=1}^{n} \theta_{n-j}^{(n)} D_2 v^j = \nabla_\tau v^n \quad \text{for } n \geqslant 1, \tag{1.10}$$

which can be derived by exchanging the summation order and using the identity (1.9).

In this work, by showing some new properties of the DOC kernels and the corresponding quadratic forms (see Lemmas 3.2–3.4), we are able to show the energy stability and a rigorous error estimate of the nonuniform BDF2 scheme for the MBE model, under the following mild time-step ratio constraint:

S1. $0 < r_k < r_s := (3 + \sqrt{17})/2 \approx 3.561$ for $2 \leqslant k \leqslant N$.

This coincides with the results in the linear case [19], and up to now seems to be the best results for nonlinear problems in the literature.

The rest of this paper is organized as follows. In Section 2, we show that the solution of the nonuniform BDF2 scheme is equivalent to the minimization problem of a convex energy functional, and thus it is uniquely solvable. Then, we present in Theorem 2.3 a discrete energy dissipation law. In Section 3, we present some new properties of the DOC kernels. This is used in Section 4 to show the L^2 norm stability and convergence property of the fully implicit scheme. Numerical experiments are presented in Section 5 to show the effectiveness of the BDF2 scheme with an adaptive time-stepping strategy. We finally give some concluding remarks in Section 6.

2 The solvability and energy stability

In this section, we show the solvability and discrete energy stability. To this end, for any grid functions $v, w \in \mathbb{V}_h$, we define the discrete L^2 inner product $\langle v, w\rangle := h^2 \sum_{\boldsymbol{x}_h \in \Omega_h} v_h w_h$ and the associated L^2 norm $\|v\| := \sqrt{\langle v, v\rangle}$. The discrete seminorms $\|\nabla_h v\|$ and $\|\Delta_h v\|$ can be defined respectively by

$$\|\nabla_h v\| := \sqrt{h^2 \sum_{\boldsymbol{x}_h \in \Omega_h} |\nabla_h v_h|^2} \quad \text{and} \quad \|\Delta_h v\| := \sqrt{h^2 \sum_{\boldsymbol{x}_h \in \Omega_h} |\Delta_h v_h|^2} \quad \text{for } v \in \mathbb{V}_h.$$

For any grid functions $v, w \in \mathbb{V}_h$, the discrete Green's formula with periodic boundary conditions yield $\langle -\nabla_h \cdot \nabla_h v, w\rangle = \langle \nabla_h v, \nabla_h w\rangle$. It is easy to verify that for $\epsilon > 0$ and $v \in \mathbb{V}_h$,

$$\|\nabla_h v\|^2 \leqslant \langle -\Delta_h v, v\rangle \leqslant \|\Delta_h v\| \cdot \|v\| \leqslant \frac{\epsilon}{2}\|\Delta_h v\|^2 + \frac{1}{2\epsilon}\|v\|^2. \tag{2.1}$$

2.1 The unique solvability

We show the solvability of the BDF2 scheme (1.7) via a discrete energy functional G on the space $\mathbb{V}_h$,

$$G[z] := \frac{1}{2} b_0^{(n)} \|z - \phi^{n-1}\|^2 + b_1^{(n)} \langle \nabla_\tau \phi^{n-1}, z\rangle + \frac{\varepsilon}{2}\|\Delta_h z\|^2 - \frac{1}{2}\langle \ln(1 + |\nabla_h z|^2), 1\rangle.$$

We have the following theorem.

Theorem 2.1. *If the time-step sizes $\tau_n \leqslant 4\varepsilon$, the BDF2 time-stepping scheme* (1.7) *is convex* [25] *and thus uniquely solvable.*

Proof. To handle the logarithmic term in the above discrete energy functional G, we consider a function $g(\lambda) := \frac{1}{2}\ln(1 + |\boldsymbol{u} + \lambda \boldsymbol{v}|^2)$ for any vectors $\boldsymbol{u}$ and $\boldsymbol{v}$ such that

$$\frac{dg(\lambda)}{d\lambda}\bigg|_{\lambda=0} = \frac{\boldsymbol{v}^{\mathrm{T}}\boldsymbol{u}}{1 + |\boldsymbol{u}|^2} = \boldsymbol{v}^{\mathrm{T}} \boldsymbol{f}(\boldsymbol{u}) \quad \text{and} \quad \frac{d^2 g(\lambda)}{d\lambda^2}\bigg|_{\lambda=0} = \frac{1 - |\boldsymbol{u}|^2}{(1 + |\boldsymbol{u}|^2)^2}\boldsymbol{v}^{\mathrm{T}}\boldsymbol{v} \leqslant \boldsymbol{v}^{\mathrm{T}}\boldsymbol{v}.$$

For any time-level index $n \geqslant 1$, the time-step condition implies $b_0^{(n)} > \frac{1}{4\varepsilon}$. Then the functional G is strictly convex as for any $\lambda \in \mathbb{R}$ and any $\psi_h \in \mathbb{V}_h$, one has

$$\frac{d^2}{d\lambda^2}G[z+\lambda\psi]\Big|_{\lambda=0} \geqslant b_0^{(n)}\|\psi\|^2 + \varepsilon\|\Delta_h\psi\|^2 - \|\nabla_h\psi\|^2 \geqslant \left(b_0^{(n)} - \frac{1}{4\varepsilon}\right)\|\psi\|^2 \geqslant 0,$$

where the inequality (2.1) with $\epsilon := 2\varepsilon$ was applied to bound $\|\nabla_h\psi\|^2$ in the above derivation. Thus, the functional G admits a unique minimizer (denoted by ϕ_h^n) if and only if it solves

$$\begin{aligned}
0 &= \frac{d}{d\lambda}G[z+\lambda\psi]\Big|_{\lambda=0} \\
&= b_0^{(n)}\langle z-\phi^{n-1},\psi\rangle + b_1^{(n)}\langle\nabla_\tau\phi^{n-1},\psi\rangle + \varepsilon\langle\Delta_h^2 z,\psi\rangle - \langle \boldsymbol{f}(\nabla_h z),\nabla_h\psi\rangle \\
&= \langle b_0^{(n)}(z-\phi^{n-1}) + b_1^{(n)}\nabla_\tau\phi^{n-1} + \varepsilon\Delta_h^2 z + \nabla_h\cdot\boldsymbol{f}(\nabla_h z),\psi\rangle.
\end{aligned}$$

This equation holds for any $\psi_h \in \mathbb{V}_h$ if and only if the unique minimizer $\phi_h^n \in \mathbb{V}_h$ solves

$$b_0^{(n)}(\phi_h^n - \phi_h^{n-1}) + b_1^{(n)}\nabla_\tau\phi_h^{n-1} + \varepsilon\Delta_h^2\phi_h^n + \nabla_h\cdot\boldsymbol{f}(\nabla_h\phi_h^n) = 0,$$

and this coincides with the BDF2 scheme (1.7). The proof is completed. □

2.2 The discrete energy dissipation law

To establish the energy stability of the BDF2 scheme (1.7), we first present the following lemma for which the proof is similar to that in [19, Lemma 2.1].

Lemma 2.2. *Suppose that* S1 *holds. Then for any non-zero sequence* $\{w_k\}_{k=1}^n$, *it holds that*

$$2w_k\sum_{j=1}^{k} b_{k-j}^{(k)} w_j \geqslant \frac{r_{k+1}}{1+r_{k+1}}\frac{w_k^2}{\tau_k} - \frac{r_k}{1+r_k}\frac{w_{k-1}^2}{\tau_{k-1}} + \left(\frac{2+4r_k-r_k^2}{1+r_k} - \frac{r_{k+1}}{1+r_{k+1}}\right)\frac{w_k^2}{\tau_k}, \quad k \geqslant 2. \tag{2.2}$$

Consequently, the discrete convolution kernels $b_{n-k}^{(n)}$ *are positive definite in the sense that*

$$\sum_{k=1}^{n} w_k\sum_{j=1}^{k} b_{k-j}^{(k)} w_j \geqslant \frac{1}{2}\sum_{k=1}^{n}\left(\frac{2+4r_k-r_k^2}{1+r_k} - \frac{r_{k+1}}{1+r_{k+1}}\right)\frac{w_k^2}{\tau_k} > 0, \quad n \geqslant 2.$$

Let $E[\phi^n]$ be the discrete version of the energy functional (1.2), i.e.,

$$E[\phi^n] := \frac{\varepsilon}{2}\|\Delta_h\phi^n\|^2 - \frac{1}{2}\langle\ln(1+|\nabla_h\phi^n|^2),1\rangle \quad \text{for } 0 \leqslant n \leqslant N. \tag{2.3}$$

We will consider the following modified discrete energy:

$$\mathcal{E}[\phi^n] := E[\phi^n] + \frac{r_{n+1}}{2(1+r_{n+1})\tau_n}\|\nabla_\tau\phi^n\|^2, \quad 0 \leqslant n \leqslant N,$$

where $\mathcal{E}[\phi^0] = E[\phi^0]$ due to $r_1 \equiv 0$. To establish an energy dissipation law, we impose a restriction of time-step sizes τ_n as follows:

$$\tau_n \leqslant 4\varepsilon\min\left\{1, \frac{2+4r_n-r_n^2}{1+r_n} - \frac{r_{n+1}}{1+r_{n+1}}\right\}, \quad n \geqslant 1. \tag{2.4}$$

We are now ready to present the following theorem.

Theorem 2.3. *Suppose that* S1 *holds with the time-step condition* (2.4). *Then the BDF*2 *scheme* (1.7) *admits the following energy dissipation law*:

$$\mathcal{E}[\phi^n] \leqslant \mathcal{E}[\phi^{n-1}] \leqslant \mathcal{E}[\phi^0] = E[\phi^0], \quad n \geqslant 1.$$

Proof. Taking the inner product of (1.7) by $\triangledown_\tau \phi^n$, one has

$$\langle D_2\phi^n, \triangledown_\tau \phi^n\rangle + \varepsilon\langle \Delta_h^2\phi^n, \triangledown_\tau \phi^n\rangle + \langle \nabla_h\cdot \boldsymbol{f}(\nabla_h\phi^n), \triangledown_\tau \phi^n\rangle = 0 \quad \text{for } n \geqslant 1. \tag{2.5}$$

By using the summation by parts argument and $2a(a-b) = a^2 - b^2 + (a-b)^2$, we obtain

$$\varepsilon\langle \Delta_h^2\phi^n, \triangledown_\tau \phi^n\rangle = \varepsilon\langle \Delta_h\phi^n, \Delta_h\triangledown_\tau \phi^n\rangle = \frac{\varepsilon}{2}\|\Delta_h\phi^n\|^2 - \frac{\varepsilon}{2}\|\Delta_h\phi^{n-1}\|^2 + \frac{\varepsilon}{2}\|\Delta_h\triangledown_\tau\phi^n\|^2. \tag{2.6}$$

To deal with the nonlinear term on the left-hand side of (2.5), we notice that for any vectors $\boldsymbol{u}$ and $\boldsymbol{v}$ one has

$$\frac{2(\boldsymbol{u}-\boldsymbol{v})^{\mathrm{T}}\boldsymbol{u}}{1+|\boldsymbol{u}|^2} = \frac{|\boldsymbol{u}|^2-|\boldsymbol{v}|^2}{1+|\boldsymbol{u}|^2} + \frac{|\boldsymbol{u}-\boldsymbol{v}|^2}{1+|\boldsymbol{u}|^2} \leqslant \ln\frac{1+|\boldsymbol{u}|^2}{1+|\boldsymbol{v}|^2} + |\boldsymbol{u}-\boldsymbol{v}|^2,$$

where the inequality $\frac{z}{1+z} \leqslant \ln(1+z)$ with $z = (|\boldsymbol{u}|^2 - |\boldsymbol{v}|^2)/(1+|\boldsymbol{v}|^2) > -1$ was used. Thus, by taking $\boldsymbol{u} := \nabla_h\phi^n$ and $\boldsymbol{v} := \nabla_h\phi^{n-1}$, one has

$$\begin{aligned}
\langle \nabla_h\cdot \boldsymbol{f}(\nabla_h\phi^n), \triangledown_\tau\phi^n\rangle &= -\langle \boldsymbol{f}(\nabla_h\phi^n), \nabla_h\triangledown_\tau\phi^n\rangle \\
&\geqslant -\frac{1}{2}\langle \ln(1+|\nabla_h\phi^n|^2), 1\rangle + \frac{1}{2}\langle \ln(1+|\nabla_h\phi^{n-1}|^2), 1\rangle - \frac{1}{2}\|\nabla_h\triangledown_\tau\phi^n\|^2 \\
&\geqslant -\frac{1}{2}\langle \ln(1+|\nabla_h\phi^n|^2), 1\rangle + \frac{1}{2}\langle \ln(1+|\nabla_h\phi^{n-1}|^2), 1\rangle \\
&\quad - \frac{\varepsilon}{2}\|\Delta_h\triangledown_\tau\phi^n\|^2 - \frac{1}{8\varepsilon}\|\triangledown_\tau\phi^n\|^2,
\end{aligned} \tag{2.7}$$

where the inequality (2.1) with $v := \triangledown_\tau\phi^n$ and $\epsilon := 2\varepsilon$ was applied to bound $\|\nabla_h\triangledown_\tau\phi^n\|^2$ in the last step. By inserting (2.6)–(2.7) into (2.5) and using together the definition (2.3), we obtain

$$\langle D_2\phi^n, \triangledown_\tau\phi^n\rangle - \frac{1}{8\varepsilon}\|\triangledown_\tau\phi^n\|^2 + E[\phi^n] - E[\phi^{n-1}] \leqslant 0 \quad \text{for } n \geqslant 1. \tag{2.8}$$

We now proceed the proof by dealing with the first term on the left-hand side of (2.8). For $n \geqslant 2$, Lemma 2.2 and the time-step condition (2.4) yield

$$\langle D_2\phi^n, \triangledown_\tau\phi^n\rangle \geqslant \frac{r_{n+1}}{2(1+r_{n+1})\tau_n}\|\triangledown_\tau\phi^n\|^2 - \frac{r_n}{2(1+r_n)\tau_{n-1}}\|\triangledown_\tau\phi^{n-1}\|^2 + \frac{1}{8\varepsilon}\|\triangledown_\tau\phi^n\|^2.$$

Then it follows from (2.8) that

$$\mathcal{E}[\phi^n] \leqslant \mathcal{E}[\phi^{n-1}], \quad n \geqslant 2.$$

For the case where $n = 1$, the fact $r_1 = 0$ and the time-step condition (2.4) yield $\tau_1 \leqslant \frac{4\varepsilon(2+r_2)}{1+r_2}$. Consequently, one has

$$\langle D_2\phi^1, \triangledown_\tau\phi^1\rangle = \frac{1}{\tau_1}\|\triangledown_\tau\phi^1\|^2 \geqslant \frac{r_2}{2(1+r_2)\tau_1}\|\triangledown_\tau\phi^1\|^2 + \frac{1}{8\varepsilon}\|\triangledown_\tau\phi^1\|^2.$$

By inserting the above inequality into (2.8), one gets $\mathcal{E}[\phi^1] \leqslant E[\phi^0] = \mathcal{E}[\phi^0]$. This completes the proof. □

Remark 2.4. By following the derivation of (1.3), we are not able to obtain the certain discrete energy dissipation law of the original energy $E[\phi^n]$ for the BDF2 scheme (1.7). With the help of Lemma 2.2, only a dissipation law of the modified energy $\mathcal{E}[\phi^n]$ is achieved. Fortunately, $\mathcal{E}[\phi^n] - E[\phi^n] \approx \tau_n\|\partial_\tau\phi^n\|^2$ so that the modified energy approximates the original energy with an order of $O(\tau_n)$. From a computational perspective, the modified discrete energy form $\mathcal{E}[\phi^n]$ suggests that small time-steps (with small step-ratios) are necessary to capture the solution behaviors when $\|\partial_t\phi\|$ becomes large, while large time-steps are acceptable to accelerate the time integration when $\|\partial_t\phi\|$ is small.

Remark 2.5. Notice that the first time-step condition in (2.4) comes from the unique solvability and the second one is necessary to maintain the discrete energy stability. In practice, the time-step constraint (2.4) requires $\tau_n = O(\varepsilon)$ which is essentially determined by the value of the surface diffusion parameter ε. Thus, the time-step condition is acceptable since the restriction $\tau_n = O(\varepsilon)$ is always required in the L^2 norm stability or convergence analysis [3, 4, 14, 20].

3 New properties of the DOC kernels

We firstly present some basic properties of the DOC kernels which can be found in [19, Lemmas 2.2 and 2.3 and Corollary 2.1].

Lemma 3.1. *Under the assumption* S1, *which implies that the discrete convolution kernels* $b_{n-k}^{(n)}$ *in* (1.6) *are positive definite, then the following properties of the DOC kernels* $\theta_{n-j}^{(n)}$ *hold*:

(i) *the discrete kernels* $\theta_{n-j}^{(n)}$ *are positive definite*;

(ii) *the discrete kernels* $\theta_{n-j}^{(n)}$ *are positive and* $\theta_{n-j}^{(n)} = \frac{1}{b_0^{(j)}}\prod_{i=j+1}^{n}\frac{r_i^2}{1+2r_i}$ *for* $1 \leqslant j \leqslant n$;

(iii) $\sum_{j=1}^{n}\theta_{n-j}^{(n)} = \tau_n$ *such that* $\sum_{k=1}^{n}\sum_{j=1}^{k}\theta_{k-j}^{(k)} = t_n$ *for* $n \geqslant 1$.

In order to facilitate the following numerical analysis, we use the BDF2 kernels $b_{k-j}^{(k)}$, the DOC kernels $\theta_{k-j}^{(k)}$ and the 2×2 identity matrix $\mathbf{I}_2$ to define the following matrices:

$$\boldsymbol{B}_2 := \begin{pmatrix} b_0^{(1)} & & & \\ b_1^{(2)} & b_0^{(2)} & & \\ & \ddots & \ddots & \\ & & b_1^{(n)} & b_0^{(n)} \end{pmatrix} \otimes \mathbf{I}_2, \quad \boldsymbol{\Theta}_2 := \begin{pmatrix} \theta_0^{(1)} & & & \\ \theta_1^{(2)} & \theta_0^{(2)} & & \\ \vdots & \vdots & \ddots & \\ \theta_{n-1}^{(n)} & \theta_{n-2}^{(n)} & \cdots & \theta_0^{(n)} \end{pmatrix} \otimes \mathbf{I}_2,$$

where "$\otimes$" denotes the tensor product. By the discrete orthogonal identity (1.9), one can verify that $\boldsymbol{\Theta}_2 = \boldsymbol{B}_2^{-1}$. Lemma 2.2 shows that the real symmetric matrix

$$\boldsymbol{B} := \boldsymbol{B}_2 + \boldsymbol{B}_2^{\mathrm{T}} \quad \text{is positive definite.} \tag{3.1}$$

Similarly, Lemma 3.1(i) implies that the real symmetric matrix $\boldsymbol{\Theta} := \boldsymbol{\Theta}_2 + \boldsymbol{\Theta}_2^{\mathrm{T}}$ is positive definite. By using (3.1), one can check that

$$\boldsymbol{\Theta} = \boldsymbol{B}_2^{-1} + (\boldsymbol{B}_2^{-1})^{\mathrm{T}} = (\boldsymbol{B}_2^{-1})^{\mathrm{T}}\boldsymbol{B}\boldsymbol{B}_2^{-1}. \tag{3.2}$$

Moreover, we define a diagonal matrix $\boldsymbol{\Lambda}_\tau := \mathrm{diag}(\sqrt{\tau_1}, \sqrt{\tau_2}, \ldots, \sqrt{\tau_n}) \otimes \mathbf{I}_2$ and

$$\widetilde{\boldsymbol{B}}_2 := \boldsymbol{\Lambda}_\tau \boldsymbol{B}_2 \boldsymbol{\Lambda}_\tau = \begin{pmatrix} \tilde{b}_0^{(1)} & & & \\ \tilde{b}_1^{(2)} & \tilde{b}_0^{(2)} & & \\ & \ddots & \ddots & \\ & & \tilde{b}_1^{(n)} & \tilde{b}_0^{(n)} \end{pmatrix} \otimes \mathbf{I}_2, \tag{3.3}$$

where the discrete kernels $\tilde{b}_0^{(k)}$ and $\tilde{b}_1^{(k)}$ are given by ($r_1 \equiv 0$)

$$\tilde{b}_0^{(k)} = \frac{1+2r_k}{1+r_k} \quad \text{and} \quad \tilde{b}_1^{(k)} = -\frac{{r_k}^{3/2}}{1+r_k} \quad \text{for } 1 \leqslant k \leqslant n.$$

By following the proof of [17, Lemma A.1], it is easy to check that the real symmetric matrix

$$\widetilde{\boldsymbol{B}} := \widetilde{\boldsymbol{B}}_2 + \widetilde{\boldsymbol{B}}_2^{\mathrm{T}} \quad \text{is positive definite.}$$

So there exists a non-singular upper triangular matrix $\boldsymbol{L}$ such that

$$\widetilde{\boldsymbol{B}} = \boldsymbol{\Lambda}_\tau \boldsymbol{B} \boldsymbol{\Lambda}_\tau = \boldsymbol{L}^{\mathrm{T}}\boldsymbol{L} \quad \text{or} \quad \boldsymbol{B} = (\boldsymbol{L}\boldsymbol{\Lambda}_\tau^{-1})^{\mathrm{T}}\boldsymbol{L}\boldsymbol{\Lambda}_\tau^{-1}. \tag{3.4}$$

We will present some discrete convolution inequalities with respect to the DOC kernels. To do so, we introduce the vector norm $\|\cdot\|$ by $\|\boldsymbol{u}\| := \sqrt{\boldsymbol{u}^{\mathrm{T}}\boldsymbol{u}}$ and the associated matrix norm $\|\boldsymbol{A}\| := \sqrt{\rho(\boldsymbol{A}^{\mathrm{T}}\boldsymbol{A})}$. Also, we define a positive quantity

$$\mathcal{M}_r := \max_{n\geqslant 1}\|\widetilde{\boldsymbol{B}}_2\|^2\|\boldsymbol{L}^{-1}\|^4 = \max_{n\geqslant 1}\frac{\lambda_{\max}(\widetilde{\boldsymbol{B}}_2^{\mathrm{T}}\widetilde{\boldsymbol{B}}_2)}{\lambda_{\min}^2(\widetilde{\boldsymbol{B}})}. \tag{3.5}$$

Under the step-ratio condition S1, a rough estimate $\mathcal{M}_r < 39$ could be followed from [17, Lemmas A.1 and A.2]. As noticed in [17, Remark 3], one has $\mathcal{M}_r \leqslant 4$ if practical simulations do not continuously use large step-ratios approaching the stability limit $r_s = 3.561$.

Lemma 3.2. *If the condition* S1 *holds, then for any vector sequences* $\boldsymbol{z}^k, \boldsymbol{w}^k \in \mathbb{R}^2$ $(1 \leqslant k \leqslant n)$,

$$\sum_{k=1}^{n}\sum_{j=1}^{k}\theta_{k-j}^{(k)}(\boldsymbol{z}^k)^{\mathrm{T}}\boldsymbol{w}^j \leqslant \frac{\epsilon}{2}\boldsymbol{z}^{\mathrm{T}}\boldsymbol{\Theta}\boldsymbol{z} + \frac{1}{2\epsilon}\boldsymbol{w}^{\mathrm{T}}\boldsymbol{B}^{-1}\boldsymbol{w} \quad \text{for any } \epsilon \geqslant 0,$$

where the vector $\boldsymbol{z} := ((\boldsymbol{z}^1)^{\mathrm{T}}, (\boldsymbol{z}^2)^{\mathrm{T}}, \dots, (\boldsymbol{z}^n)^{\mathrm{T}})^{\mathrm{T}}$ *and* $\boldsymbol{w} := ((\boldsymbol{w}^1)^{\mathrm{T}}, (\boldsymbol{w}^2)^{\mathrm{T}}, \dots, (\boldsymbol{w}^n)^{\mathrm{T}})^{\mathrm{T}}$.

Proof. This result can be verified by following from the proof of [17, Lemma A.3]. □

Lemma 3.3 (See [14, Lemma 3.5])**.** *For any* $\boldsymbol{v}, \boldsymbol{w} \in \mathbb{R}^2$, *there exists a symmetric matrix* $\boldsymbol{Q}_f \in \mathbb{R}^{2\times 2}$ *such that* $\boldsymbol{f}(\boldsymbol{v}) - \boldsymbol{f}(\boldsymbol{w}) = \boldsymbol{Q}_f(\boldsymbol{v} - \boldsymbol{w})$, *and the eigenvalues of* $\boldsymbol{Q}_f$ *satisfy* $\lambda_1, \lambda_2 \in [-1/8, 1]$. *Consequently, it holds that*

$$|\boldsymbol{f}(\boldsymbol{v}) - \boldsymbol{f}(\boldsymbol{w})| \leqslant |\boldsymbol{v} - \boldsymbol{w}| \quad \text{for any } \boldsymbol{v}, \boldsymbol{w} \in \mathbb{R}^2.$$

Lemma 3.4. *Assume that the condition* S1 *holds. For any vector sequences* $\boldsymbol{v}^k, \boldsymbol{z}^k, \boldsymbol{w}^k \in \mathbb{R}^2$, $1 \leqslant k \leqslant n$ *and any* $\epsilon > 0$, *it holds that*

$$\sum_{k=1}^{n}\sum_{j=1}^{k}\theta_{k-j}^{(k)}(\boldsymbol{z}^k)^{\mathrm{T}}[\boldsymbol{f}(\boldsymbol{v}^j + \boldsymbol{w}^j) - \boldsymbol{f}(\boldsymbol{v}^j)] \leqslant \sum_{k=1}^{n}\sum_{j=1}^{k}\theta_{k-j}^{(k)}\left[\epsilon(\boldsymbol{z}^k)^{\mathrm{T}}\boldsymbol{z}^j + \frac{\mathcal{M}_r}{\epsilon}(\boldsymbol{w}^k)^{\mathrm{T}}\boldsymbol{w}^j\right],$$

where the positive constant $\mathcal{M}_r$, *independent of the time* t_n, *time-step sizes* τ_n *and time-step ratios* r_n, *is defined by* (3.5). *Consequently,*

$$\sum_{k=1}^{n}\sum_{j=1}^{k}\theta_{k-j}^{(k)}(\boldsymbol{z}^k)^{\mathrm{T}}[\boldsymbol{f}(\boldsymbol{v}^j + \boldsymbol{z}^j) - \boldsymbol{f}(\boldsymbol{v}^j)] \leqslant 2\sqrt{\mathcal{M}_r}\sum_{k=1}^{n}\sum_{j=1}^{k}\theta_{k-j}^{(k)}(\boldsymbol{z}^k)^{\mathrm{T}}\boldsymbol{z}^j.$$

Proof. According to Lemma 3.3, there exists a sequence of symmetric matrices

$$\boldsymbol{Q}_f^j \in \mathbb{R}^{2\times 2} \quad \text{such that} \quad \boldsymbol{f}(\boldsymbol{w}^j + \boldsymbol{v}^j) - \boldsymbol{f}(\boldsymbol{w}^j) = \boldsymbol{Q}_f^j\boldsymbol{v}^j \quad \text{for } 1 \leqslant j \leqslant n,$$

where the corresponding eigenvalues of $\boldsymbol{Q}_f^j$ satisfy $\lambda_{j1}, \lambda_{j2} \in [-1/8, 1]$ for $1 \leqslant j \leqslant n$. Now we define the following symmetric matrix:

$$\boldsymbol{Q} := \mathrm{diag}(\boldsymbol{Q}_f^1, \boldsymbol{Q}_f^2, \dots, \boldsymbol{Q}_f^n) \in \mathbb{R}^{2n\times 2n}.$$

The eigenvalues μ_k of $\boldsymbol{Q}_{2n\times 2n}$ satisfy $\mu_k \in [-1/8, 1]$ for $1 \leqslant k \leqslant 2n$. Thus

$$\rho(\boldsymbol{Q}) \leqslant 1 \quad \text{such that} \quad \|\boldsymbol{Q}\| \leqslant 1. \tag{3.6}$$

Also, it is easy to verify that $\boldsymbol{Q}$ and $\boldsymbol{\Lambda}_\tau$ are commutative, i.e., $\boldsymbol{Q}\boldsymbol{\Lambda}_\tau = \boldsymbol{\Lambda}_\tau\boldsymbol{Q}$.

By introducing $\boldsymbol{z}_e := ((\boldsymbol{z}^1)^{\mathrm{T}}, (\boldsymbol{z}^2)^{\mathrm{T}}, \dots, (\boldsymbol{z}^n)^{\mathrm{T}})^{\mathrm{T}}$ and $\boldsymbol{w}_e := ((\boldsymbol{w}^1)^{\mathrm{T}}, (\boldsymbol{w}^2)^{\mathrm{T}}, \dots, (\boldsymbol{w}^n)^{\mathrm{T}})^{\mathrm{T}}$, we apply Lemma 3.2 with $\boldsymbol{z} := \boldsymbol{z}_e$ and $\boldsymbol{w} := \boldsymbol{Q}\boldsymbol{w}_e$ to derive that

$$\begin{aligned}\sum_{k=1}^{n}\sum_{j=1}^{k}\theta_{k-j}^{(k)}(\boldsymbol{z}^k)^{\mathrm{T}}[\boldsymbol{f}(\boldsymbol{v}^j + \boldsymbol{w}^j) - \boldsymbol{f}(\boldsymbol{v}^j)] &= \sum_{k=1}^{n}\sum_{j=1}^{k}\theta_{k-j}^{(k)}(\boldsymbol{z}^k)^{\mathrm{T}}\boldsymbol{Q}_f^j\boldsymbol{w}^j \\ &\leqslant \frac{\epsilon}{2}\boldsymbol{z}_e^{\mathrm{T}}\boldsymbol{\Theta}\boldsymbol{z}_e + \frac{1}{2\epsilon}\boldsymbol{w}_e^{\mathrm{T}}\boldsymbol{Q}^{\mathrm{T}}\boldsymbol{B}^{-1}\boldsymbol{Q}\boldsymbol{w}_e \\ &= \epsilon\sum_{k=1}^{n}\sum_{j=1}^{k}\theta_{k-j}^{(k)}(\boldsymbol{z}^k)^{\mathrm{T}}\boldsymbol{z}^j + \frac{1}{2\epsilon}\boldsymbol{w}_e^{\mathrm{T}}\boldsymbol{Q}^{\mathrm{T}}\boldsymbol{B}^{-1}\boldsymbol{Q}\boldsymbol{w}_e.\end{aligned} \tag{3.7}$$

Now we deal with the second term on the right-hand side of the above inequality. It follows from (3.2) and (3.4) that

$$\boldsymbol{\Theta} = (\boldsymbol{B}_2^{-1})^{\mathrm{T}}\boldsymbol{B}\boldsymbol{B}_2^{-1} = (\boldsymbol{B}_2^{-1})^{\mathrm{T}}(\boldsymbol{L}\boldsymbol{\Lambda}_\tau^{-1})^{\mathrm{T}}\boldsymbol{L}\boldsymbol{\Lambda}_\tau^{-1}\boldsymbol{B}_2^{-1} = (\boldsymbol{L}\boldsymbol{\Lambda}_\tau^{-1}\boldsymbol{B}_2^{-1})^{\mathrm{T}}\boldsymbol{L}\boldsymbol{\Lambda}_\tau^{-1}\boldsymbol{B}_2^{-1},$$

and then $\boldsymbol{w}_e^{\mathrm{T}}\boldsymbol{\Theta}\boldsymbol{w}_e = \|\boldsymbol{L}\boldsymbol{\Lambda}_\tau^{-1}\boldsymbol{B}_2^{-1}\boldsymbol{w}_e\|^2$. We use the definition (3.3) and the equality (3.4) to derive that

$$\begin{aligned}
\boldsymbol{w}_e^{\mathrm{T}}\boldsymbol{Q}^{\mathrm{T}}\boldsymbol{B}^{-1}\boldsymbol{Q}\boldsymbol{w}_e &= ((\boldsymbol{L}^{-1})^{\mathrm{T}}\boldsymbol{\Lambda}_\tau\boldsymbol{Q}\boldsymbol{w}_e)^{\mathrm{T}}(\boldsymbol{L}^{-1})^{\mathrm{T}}\boldsymbol{\Lambda}_\tau\boldsymbol{Q}\boldsymbol{w}_e = \|(\boldsymbol{L}^{-1})^{\mathrm{T}}\boldsymbol{\Lambda}_\tau\boldsymbol{Q}\boldsymbol{w}_e\|^2\\
&= \|(\boldsymbol{L}^{-1})^{\mathrm{T}}\boldsymbol{\Lambda}_\tau\boldsymbol{Q}\boldsymbol{B}_2\boldsymbol{\Lambda}_\tau\boldsymbol{L}^{-1}\boldsymbol{L}\boldsymbol{\Lambda}_\tau^{-1}\boldsymbol{B}_2^{-1}\boldsymbol{w}_e\|^2\\
&\leqslant \|(\boldsymbol{L}^{-1})^{\mathrm{T}}\boldsymbol{\Lambda}_\tau\boldsymbol{Q}\boldsymbol{B}_2\boldsymbol{\Lambda}_\tau\boldsymbol{L}^{-1}\|^2\|\boldsymbol{L}\boldsymbol{\Lambda}_\tau^{-1}\boldsymbol{B}_2^{-1}\boldsymbol{w}_e\|^2\\
&= \|(\boldsymbol{L}^{-1})^{\mathrm{T}}\boldsymbol{Q}\widetilde{\boldsymbol{B}}_2\boldsymbol{L}^{-1}\|^2\cdot\boldsymbol{w}_e^{\mathrm{T}}\boldsymbol{\Theta}\boldsymbol{w}_e\\
&\leqslant \|\boldsymbol{Q}\|\|\widetilde{\boldsymbol{B}}_2\|\|\boldsymbol{L}^{-1}\|^4\cdot\boldsymbol{w}_e^{\mathrm{T}}\boldsymbol{\Theta}\boldsymbol{w}_e\\
&\leqslant 2\mathcal{M}_r\sum_{k=1}^{n}\sum_{j=1}^{k}\theta_{k-j}^{(k)}(\boldsymbol{w}^k)^{\mathrm{T}}\boldsymbol{w}^j,
\end{aligned}$$

where the estimate (3.6) and the definition (3.5) of $\mathcal{M}_r$ have been used in the last inequality. Inserting the above inequality into (3.7), we obtain the claimed first inequality. The second result then follows immediately by setting $\boldsymbol{w}^j = \boldsymbol{z}^j$ and $\epsilon := \sqrt{\mathcal{M}_r}$. □

4 The L^2 norm stability and convergence analysis

In this section, we shall show the L^2 norm stability and convergence analysis of the variable-step BDF2 scheme for the MBE model. Always, they need a discrete Grönwall's inequality [19, Lemma 3.1].

Lemma 4.1. *Let $\lambda \geqslant 0$, and the time sequences $\{\xi_k\}_{k=0}^N$ and $\{V_k\}_{k=1}^N$ be nonnegative. If*

$$V_n \leqslant \lambda\sum_{j=1}^{n-1}\tau_j V_j + \sum_{j=0}^{n}\xi_j \quad \text{for } 1 \leqslant n \leqslant N,$$

then it holds that

$$V_n \leqslant \exp(\lambda t_{n-1})\sum_{j=0}^{n}\xi_j \quad \text{for } 1 \leqslant n \leqslant N.$$

4.1 The L^2 norm stability

We first show the L^2 norm stability. In what follows, for notation simplicity, we shall set

$$\sum_{k,j} := \sum_{k=1}^{n}\sum_{j=1}^{k}.$$

Theorem 4.2. *If* S1 *holds with the time-step condition $\tau_n \leqslant \varepsilon/(16\mathcal{M}_r^2)$, the variable-step BDF*2 *scheme* (1.7) *is stable in the L^2 norm with respect to small initial disturbance, namely,*

$$\|\bar{\phi}^n - \phi^n\| \leqslant 2\exp(16\mathcal{M}_r^2 t_{n-1}/\varepsilon)\|\bar{\phi}^0 - \phi^0\| \quad \text{for } 1 \leqslant n \leqslant N,$$

where $\bar{\phi}_h^n$ solves the equation (1.7) *with the initial data $\bar{\phi}_h^0$.*

Proof. Let z_h^k be the solution perturbation $z_h^k := \bar{\phi}_h^k - \phi_h^k$ for $\boldsymbol{x}_h \in \bar{\Omega}_h$ and $0 \leqslant k \leqslant N$. Then it is easy to obtain the perturbed equation

$$D_2 z_h^j + \varepsilon\Delta_h^2 z_h^j + \nabla_h\cdot(\boldsymbol{f}(\nabla_h\bar{\phi}_h^j) - \boldsymbol{f}(\nabla_h\phi_h^j)) = 0 \quad \text{for } \boldsymbol{x}_h \in \Omega_h \quad \text{and} \quad 1 \leqslant j \leqslant N. \tag{4.1}$$

Multiplying both sides of (4.1) by the DOC kernels $\theta_{k-j}^{(k)}$, and summing up from 1 to k, we have

$$\nabla_\tau z_h^k + \varepsilon\sum_{j=1}^{k}\theta_{k-j}^{(k)}\Delta_h^2 z_h^j + \sum_{j=1}^{k}\theta_{k-j}^{(k)}\nabla_h\cdot[\boldsymbol{f}(\nabla_h\bar{\phi}_h^j) - \boldsymbol{f}(\nabla_h\phi_h^j)] = 0,$$

where the equality (1.10) has been used in the derivation. Now by taking the inner product of the above equality with $2z^k$, and summing up the derived equality from $k=1$ to n, one obtains

$$\|z^n\|^2 - \|z^0\|^2 + 2\varepsilon \sum_{k,j} \theta_{k-j}^{(k)} \langle \Delta_h z^j, \Delta_h z^k \rangle \leqslant 2 \sum_{k,j} \theta_{k-j}^{(k)} \langle \boldsymbol{f}(\nabla_h \bar{\phi}^j) - \boldsymbol{f}(\nabla_h \phi^j), \nabla_h z^k \rangle. \tag{4.2}$$

Now, by taking $\boldsymbol{v}^k := \nabla_h \phi^j$ and $\boldsymbol{z}^k := \nabla_h z^k$ in the second inequality of Lemma 3.4, one has

$$\begin{aligned} \mathfrak{F}(\phi^n, z^n) &:= 2 \sum_{k,j} \theta_{k-j}^{(k)} \langle \boldsymbol{f}(\nabla_h \phi^j + \nabla_h z^j) - \boldsymbol{f}(\nabla_h \phi^j), \nabla_h z^k \rangle \\ &\leqslant 4\sqrt{\mathcal{M}_r} \sum_{k,j} \theta_{k-j}^{(k)} \langle \nabla_h z^j, \nabla_h z^k \rangle = 4\sqrt{\mathcal{M}_r} \sum_{k,j} \theta_{k-j}^{(k)} \langle -\Delta_h z^k, z^j \rangle. \end{aligned} \tag{4.3}$$

Note that Lemma 3.4 holds for the simplest case where $\boldsymbol{f}(\boldsymbol{v}) := \boldsymbol{v}$. Thus one can take $\boldsymbol{z}^k := -\Delta_h z^k$, $\boldsymbol{w}^j := z^j$ and $\epsilon = \varepsilon/(2\sqrt{\mathcal{M}_r})$ to obtain

$$\mathfrak{F}(\phi^n, z^n) \leqslant 2\varepsilon \sum_{k,j} \theta_{k-j}^{(k)} \langle \Delta_h z^j, \Delta_h z^k \rangle + 8\varepsilon^{-1} \mathcal{M}_r^2 \sum_{k,j} \theta_{k-j}^{(k)} \langle z^j, z^k \rangle. \tag{4.4}$$

It follows from (4.2) and (4.4) that

$$\|z^n\|^2 \leqslant \|z^0\|^2 + 8\varepsilon^{-1} \mathcal{M}_r^2 \sum_{k,j} \theta_{k-j}^{(k)} \langle z^j, z^k \rangle \leqslant \|z^0\|^2 + 8\varepsilon^{-1} \mathcal{M}_r^2 \sum_{k,j} \theta_{k-j}^{(k)} \|z^j\| \|z^k\|$$

for $1 \leqslant n \leqslant N$. Now by choosing some integer n_1 $(0 \leqslant n_1 \leqslant n)$ such that $\|z^{n_1}\| = \max_{0 \leqslant k \leqslant n} \|z^k\|$, and setting $n = n_1$ in the above inequality, we obtain by using Lemma 3.1(iii)

$$\|z^n\| \leqslant \|z^{n_1}\| \leqslant \|z^0\| + 8\varepsilon^{-1} \mathcal{M}_r^2 \sum_{k=1}^{n_1} \tau_k \|z^k\| \leqslant \|z^0\| + 8\varepsilon^{-1} \mathcal{M}_r^2 \sum_{k=1}^{n} \tau_k \|z^k\| \tag{4.5}$$

for $1 \leqslant n \leqslant N$. By noticing the time-step condition $\tau_n \leqslant \varepsilon/(16\mathcal{M}_r^2)$, one gets from (4.5) that

$$\|z^n\| \leqslant 2\|z^0\| + 16\varepsilon^{-1} \mathcal{M}_r^2 \sum_{k=1}^{n-1} \tau_k \|z^k\| \quad \text{for } 1 \leqslant n \leqslant N.$$

Then the desired result follows by using the discrete Grönwall's inequality in Lemma 4.1. $\square$

Notice that Theorem 4.2 does not involve any undesirable unbounded factors, such as C_r or Γ_n in the existing works [2,5,8]. For the time $t_n \leqslant T$, the stability factor $\exp(16\mathcal{M}_r^2 t_{n-1}/\varepsilon)$ remains bounded as the time-steps τ_n vanish or the step-ratios r_n approach the zero-stability limit $r_s = 3.561$. Thus Theorem 4.2 also shows that the variable-step BDF2 time-stepping scheme is robustly stable with respect to the variation of time-step sizes. Now by taking $\bar{\phi}_h^0 = 0$ in Theorem 4.2 and using together Theorem 2.1, we have the following corollary which simulates the L^2 norm estimate (1.4).

Corollary 4.3. *If* S1 *holds, the solution of the variable-step BDF*2 *scheme* (1.7) *fulfills*

$$\|\phi^n\| \leqslant \frac{1}{1-\delta} \exp\left(\frac{8\mathcal{M}_r^2 t_{n-1}}{(1-\delta)\varepsilon}\right) \|\phi^0\| \quad \textit{for } \tau_n \leqslant \frac{\delta\varepsilon}{8\mathcal{M}_r^2} \ (0 < \delta < 1) \quad \textit{and} \quad 1 \leqslant n \leqslant N.$$

4.2 L^2 norm error estimates

We are now at the stage to give the error estimates of the variable-step BDF2 scheme. To do this, let $\xi^j := D_2\Phi(t_j) - \partial_t \Phi(t_j)$ be the local consistency error of the BDF2 scheme at the time $t = t_j$. We will consider a convolutional consistency error Ξ^k defined by

$$\Xi^k := \sum_{j=1}^{k} \theta_{k-j}^{(k)} \xi^j = \sum_{j=1}^{k} \theta_{k-j}^{(k)} (D_2\Phi(t_j) - \partial_t \Phi(t_j)) \quad \text{for } k \geqslant 1. \tag{4.6}$$

Lemma 4.4 (See [17, Lemma 3.4]). *If* S1 *holds, the consistency error* Ξ^k *in* (4.6) *satisfies*

$$|\Xi^k| \leqslant \theta_{k-1}^{(k)} \int_0^{t_1} |\Phi''(t)| dt + 3 \sum_{j=1}^{k} \theta_{k-j}^{(k)} \tau_j \int_{t_{j-1}}^{t_j} |\Phi'''(t)| dt \quad \text{for } k \geqslant 1$$

such that

$$\sum_{k=1}^{n} |\Xi^k| \leqslant \tau_1 \int_0^{t_1} |\Phi''(t)| dt \sum_{k=1}^{n} \prod_{i=2}^{k} \frac{r_i^2}{1+2r_i} + 3t_n \max_{1 \leqslant j \leqslant n} \left(\tau_j \int_{t_{j-1}}^{t_j} |\Phi'''(t)| dt \right) \quad \text{for } n \geqslant 1.$$

Hereafter, we shall use a generic constant $C_\phi > 0$ in the error estimates which is not necessarily the same at different occurrences, but always independent of the time-steps τ_n, the step-ratios r_n and the spatial length h.

Theorem 4.5. *Assume that the MBE problem* (1.1) *has a smooth solution* $\Phi \in C_{\boldsymbol{x},t}^{(6,3)}(\Omega \times (0,T])$. *If* S1 *holds with the time-steps* $\tau_n \leqslant \varepsilon/(16\mathcal{M}_r^2)$, *the BDF2 scheme* (1.7) *admits the following error estimate*:

$$\|\Phi^n - \phi^n\| \leqslant C_\phi \exp(16\mathcal{M}_r^2 t_{n-1}/\varepsilon) \left[\tau_1^2 \sum_{k=1}^{n} \prod_{i=2}^{k} \frac{r_i^2}{1+2r_i} + t_n(\tau^2 + h^2) \right] \quad \text{for } 1 \leqslant n \leqslant N.$$

Proof. Let $\Phi_h^n := \Phi(\boldsymbol{x}_h, t_n)$ and e_h^n be the error function $e_h^n := \Phi_h^n - \phi_h^n$ with $e_h^n := 0$ for $\boldsymbol{x}_h \in \bar{\Omega}_h$. We then have the following error equation:

$$D_2 e_h^j + \varepsilon \Delta_h^2 e_h^j + \nabla_h \cdot [\boldsymbol{f}(\nabla_h \Phi_h^j) - \boldsymbol{f}(\nabla_h \phi_h^j)] = \xi_h^j + \eta_h^j, \tag{4.7}$$

where ξ_h^j and η_h^j are the local consistency error in time and physical domain, respectively. If the solution is smooth, Lemma 3.1(iii) gives

$$\sum_{k=1}^{n} \|\Pi^k\| \leqslant C_\phi t_n h^2 \quad \text{for } 1 \leqslant n \leqslant N, \quad \text{where } \Pi_h^k := \sum_{j=1}^{k} \theta_{k-j}^{(k)} \eta_h^j. \tag{4.8}$$

Multiplying both sides of (4.7) by the DOC kernels $\theta_{k-j}^{(k)}$, and summing up the superscript from $j = 1$ to k, we obtain by applying the equality (1.10)

$$\triangledown_\tau e_h^k + \varepsilon \sum_{j=1}^{k} \theta_{k-j}^{(k)} \Delta_h^2 e_h^j + \sum_{j=1}^{k} \theta_{k-j}^{(k)} \nabla_h \cdot [\boldsymbol{f}(\nabla_h \Phi_h^j) - \boldsymbol{f}(\nabla_h \phi_h^j)] = \Xi_h^k + \Pi_h^k,$$

where Ξ_h^k and Π_h^k are defined by (4.6) and (4.8), respectively. Now by taking the inner product of the above equality with $2e^k$, and summing up the superscript from $k = 1$ to n, we obtain by using the discrete Green's formula

$$\|e^n\|^2 - \|e^0\|^2 + 2\varepsilon \sum_{k,j} \theta_{k-j}^{(k)} \langle \Delta_h e^j, \Delta_h e^k \rangle \leqslant \mathfrak{F}(\phi^n, e^n) + 2 \sum_{k=1}^{n} \langle \Xi^k + \Pi^k, e^k \rangle, \tag{4.9}$$

where $\mathfrak{F}(\phi^n, e^n)$ is defined in (4.3). The derivation of (4.4) yields

$$\mathfrak{F}(\phi^n, e^n) \leqslant 2\varepsilon \sum_{k,j} \theta_{k-j}^{(k)} \langle \Delta_h e^j, \Delta_h e^k \rangle + 8\varepsilon^{-1} \mathcal{M}_r^2 \sum_{k,j} \theta_{k-j}^{(k)} \langle e^j, e^k \rangle.$$

With the help of the Cauchy-Schwarz inequality, it follows from (4.9) that

$$\|e^n\|^2 \leqslant \|e^0\|^2 + 8\varepsilon^{-1} \mathcal{M}_r^2 \sum_{k,j} \theta_{k-j}^{(k)} \|e^j\| \|e^k\| + 2 \sum_{k=1}^{n} \|\Xi^k + \Pi^k\| \|e^k\| \quad \text{for } 1 \leqslant n \leqslant N. \tag{4.10}$$

Then, by choosing some integer n_2 $(0 \leqslant n_2 \leqslant n)$ such that $\|e^{n_2}\| = \max_{0\leqslant k\leqslant n}\|e^k\|$, and setting $n = n_2$ in the above inequality (4.10), we obtain by using together Lemma 3.1(iii) and the time-step condition $\tau_n \leqslant \varepsilon/(16\mathcal{M}_r^2)$

$$\|e^n\| \leqslant 2\|e^0\| + 16\varepsilon^{-1}\mathcal{M}_r^2\sum_{k=1}^{n-1}\tau_k\|e^k\| + 4\sum_{k=1}^{n}\|\Xi^k + \Pi^k\| \quad \text{for } 1 \leqslant n \leqslant N.$$

Then by the discrete Grönwall's inequality in Lemma 4.1 we have

$$\|e^n\| \leqslant 2\exp(16\mathcal{M}_r^2 t_{n-1}/\varepsilon)\left(\|e^0\| + 2\sum_{k=1}^{n}\|\Xi^k\| + 2\sum_{k=1}^{n}\|\Pi^k\|\right) \quad \text{for } 1 \leqslant n \leqslant N.$$

The desired result follows by using together the estimates in (4.8) and Lemma 4.4. □

Notice that Theorem 4.5 confirms at least a first-order convergence rate of the numerical solution under the step-ratio condition S1, as $\tau_1\sum_{k=1}^{n}\prod_{i=2}^{k}\frac{r_i^2}{1+2r_i} \leqslant t_n$. The second-order rate of convergence can be recovered if the following assumption is fulfilled:

S2. The time-step ratios r_k are contained in S1, but almost all of them are less than $1+\sqrt{2}$, or $|\mathfrak{R}| = N_0 \ll N$, where $\mathfrak{R}$ is an index set $\mathfrak{R} := \{k \mid 1+\sqrt{2} \leqslant r_k < (3+\sqrt{17})/2\}$.

Although the condition S1 allows one to use a series of increasing time-steps with the amplification factors up to 3.561, while in practice, the use of large time-steps will result in a loss of the numerical accuracy. In this sense, the condition S2 is much more reasonable because large amplification factors of the time-step size rarely appear continuously in long-time simulations. As shown in [19, Lemma 3.3], there exists a step-ratio-dependent constant c_r such that $\sum_{k=1}^{n}\prod_{i=2}^{k}\frac{r_i^2}{1+2r_i} \leqslant c_r$. This results in the following corollary.

Corollary 4.6. *Assume that the nonlinear MBE problem* (1.1) *has a unique smooth solution. If the step-ratio assumption* S2 *holds with the time-steps* $\tau_n \leqslant \varepsilon/(16\mathcal{M}_r^2)$*, the BDF*2 *scheme* (1.7) *is second-order convergent in the* L^2 *norm,*

$$\|\Phi^n - \phi^n\| \leqslant C_\phi\exp(16\mathcal{M}_r^2 t_{n-1}/\varepsilon)(c_r\tau_1^2 + t_n(\tau^2+h^2)) \quad \textit{for } 1 \leqslant n \leqslant N.$$

5 Numerical examples

In this section, we shall present some numerical experiments by using generic MATLAB on a Windows7 platform with 2 GHz CPU and 6GB of RAM. In all our computations, a fixed-point iteration scheme is employed to solve the nonlinear BDF2 scheme at each time level with a tolerance 10^{-12}.

5.1 Random generated time meshes

We first test the performance on random generated time meshes. To this end, we set $\varepsilon = 0.1$ and consider the following exterior-forced MBE model:

$$\Phi_t = -\varepsilon\Delta^2\Phi - \nabla\cdot\boldsymbol{f}(\nabla\Phi) + g(x,y,t), \quad \Omega = (0,2\pi)^2.$$

The function $g(x,y,t)$ is chosen such that the exact solution yields $\Phi(x,y,t) = \cos(t)\sin(x)\sin(y)$. The accuracy of the variable-step BDF2 scheme is tested via the random meshes. We take

$$\tau_k := T\sigma_k/S, \quad 1 \leqslant k \leqslant N,$$

where $\sigma_k \in (0,1)$ is a uniformly distributed random number and $S = \Sigma_{k=1}^N\sigma_k$. The discrete error in the L^2 norm will be tested: $e(N) := \|\Phi(T) - \phi^N\|$, and the following convergence rate will be reported:

$$\text{Order} \approx \log(e(N)/e(2N))/\log(\tau(N)/\tau(2N)),$$

where $\tau(N)$ denotes the maximal time-step size for total N subintervals.

Table 1 Accuracy of the BDF2 scheme (1.7) on the random time mesh

N	τ	$e(N)$	Order	$\max r_k$	N_1
10	1.49E−01	1.23E−01	–	2.94	0
20	9.16E−02	8.20E−02	1.84	11.98	3
40	5.52E−02	2.57E−02	2.29	34.82	7
80	2.70E−02	4.78E−03	2.35	37.72	13
160	1.23E−02	7.20E−04	2.42	71.89	24
320	6.26E−03	1.85E−04	2.00	850.80	49

In this example, we use 3,000 grid points in the physical domain and solve the problem until $T = 1$. The numerical results are tabulated in Table 1, in which we have also recorded the maximal time-step size τ, the maximal step-ratio and the number (denoted by N_1 in Table 1) of time levels with the step-ratio $r_k \geqslant (3+\sqrt{17})/2$. It is clearly seen that the BDF2 scheme possesses a second-order rate of convergence for those nonuniform time meshes.

5.2 Adaptive time-stepping strategy

Algorithm 1 Adaptive time-stepping strategy

Require: Given ϕ^n and time-step τ_n;

1: Compute ϕ_1^{n+1} by using the BDF1 scheme with time-step τ_n.
2: Compute ϕ_2^{n+1} by using the BDF2 scheme with time-step τ_n.
3: Calculate $e_{n+1} = \|\phi_2^{n+1} - \phi_1^{n+1}\|/\|\phi_2^{n+1}\|$.
4: **if** $e_{n+1} < \text{tol}$ or $\tau_n \leqslant \tau_{\min}$ **then**
5:     **if** $e_{n+1} < \text{tol}$ **then**
6:         Update time-step size $\tau_{n+1} \leftarrow \min\{\max\{\tau_{\min}, \tau_{\text{ada}}\}, \tau_{\max}\}$.
7:     **else**
8:         Update time-step size $\tau_{n+1} \leftarrow \tau_{\min}$.
9:     **end if**
10: **else**
11:     Recalculate with time-step size $\tau_n \leftarrow \min\{\max\{\tau_{\min}, \tau_{\text{ada}}\}, \tau_{\max}\}$; Goto 1.
12: **end if**

In what follows, we test a practical adaptive time-stepping strategy proposed in [11]. In addition, several adaptive time-stepping strategies can also be found in [21,27]. As verified in the previous sections, the variable-step BDF2 scheme (1.7) is robustly stable with respect to the step-size variations satisfying the step-ratio condition S1. In [11], the adaptive time-step τ_{ada} (the next step) is updated adaptively by using the current step information τ_{cur} via the following formula:

$$\tau_{\text{ada}}(e, \tau_{\text{cur}}) = \min\{S_a\sqrt{\text{tol}/e}\,\tau_{\text{cur}}, r_s\tau_{\text{cur}}\},$$

where e is the relative error of the solution at the current time-level, tol is a reference tolerance, and S_a is some default safety parameter determined by try-and-error tests. Notice that $r_s = 3.561$ is an artificial constant that is due to the condition S1. More details of the above adaptive time-stepping strategy can be found in Algorithm 1. In our computations, if not explicitly specified, we choose the safety coefficient as $S_a = 0.9$, and set the reference tolerance $\text{tol} = 10^{-3}$. The maximal time-step is chosen as $\tau_{\max} = 0.1$ while the minimal time-step is set to be $\tau_{\min} = 10^{-4}$.

In this example, we consider the MBE model (1.1) with the following initial condition:

$$\phi_0(x, y) = 0.1(\sin 3x \sin 2y + \sin 5x \sin 5y). \tag{5.1}$$

We take the parameter $\varepsilon = 0.1$ and use 128×128 uniform meshes in the physical domain $\Omega = (0, 2\pi)^2$. To obtain the deviation of the height function, we define the roughness measure function $R(t)$ as follows:

$$R(t) = \sqrt{\frac{1}{|\Omega|}\int_\Omega (\phi(\boldsymbol{x}, t) - \bar{\phi}(\boldsymbol{x}, t))^2 d\boldsymbol{x}},$$

where $\bar{\phi}(t) = \frac{1}{|\Omega|}\int_\Omega \phi(\boldsymbol{x}, t)d\boldsymbol{x}$ is the average.

We aim at simulating the benchmark problem with the initial condition of (5.1). We first test the efficiency and accuracy of the adaptive time-stepping stretchy Algorithm 1. To make a comparison, we carry out the numerical simulation until time $T = 30$ by using a uniform time mesh. Subsequently, we employ the adaptive strategy described in Algorithm 1 to repeat the simulation. The numerical results are summarized in Figure 1. We note that it takes 30,000 uniform time-steps (with the CPU time 1,914.47 seconds) with $\tau = 10^{-3}$, while the total number of adaptive time-steps is only 529 (107.71 seconds) to get the similar results. Consequently, one can find that the time-stepping adaptive strategy is computationally efficient. In addition, the right subplot in Figure 1 shows that the adaptive step-ratios satisfy the condition S1 during the current adaptive computation.

The evolutions of the numerical solutions obtained by using the adaptive time-stepping strategy are depicted in Figure 2. Correspondingly, the evolutions of the energy, the roughness and the adaptive time-steps for the MBE model are summarized in Figure 3, demonstrating a very good agreement with the existing works [16, 20, 21]. In order to see the numerical performance, we use the same initial data with different parameters $\epsilon = 0.20$, $\epsilon = 0.10$ and $\epsilon = 0.05$ to carry out the simulations. The energy curves and the correspondingly adaptive steps are summarized in Figure 4. We observe that the variable-step BDF2 scheme (1.7) with the adaptive settings $\tau_{\max} = 0.1$ and $\tau_{\min} = 10^{-4}$ can work well for the current numerical simulations.

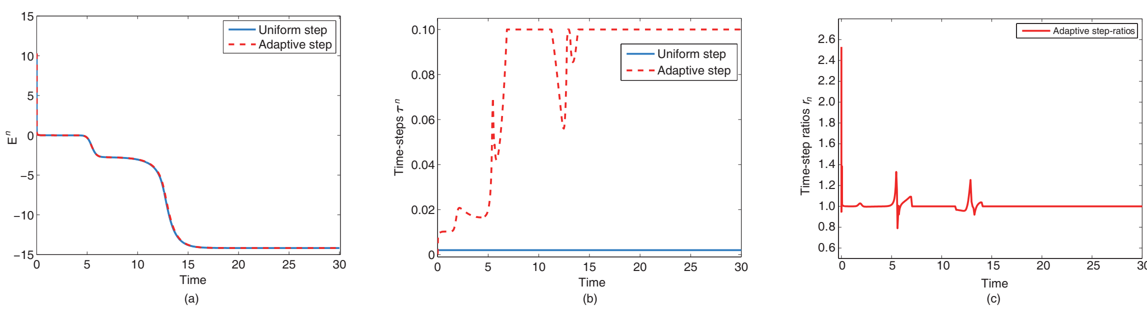

Figure 1 (Color online) Evolutions of energy (a), time-steps (b) and time-step ratios (c) of the MBE equation by using different time strategies until time $T = 30$

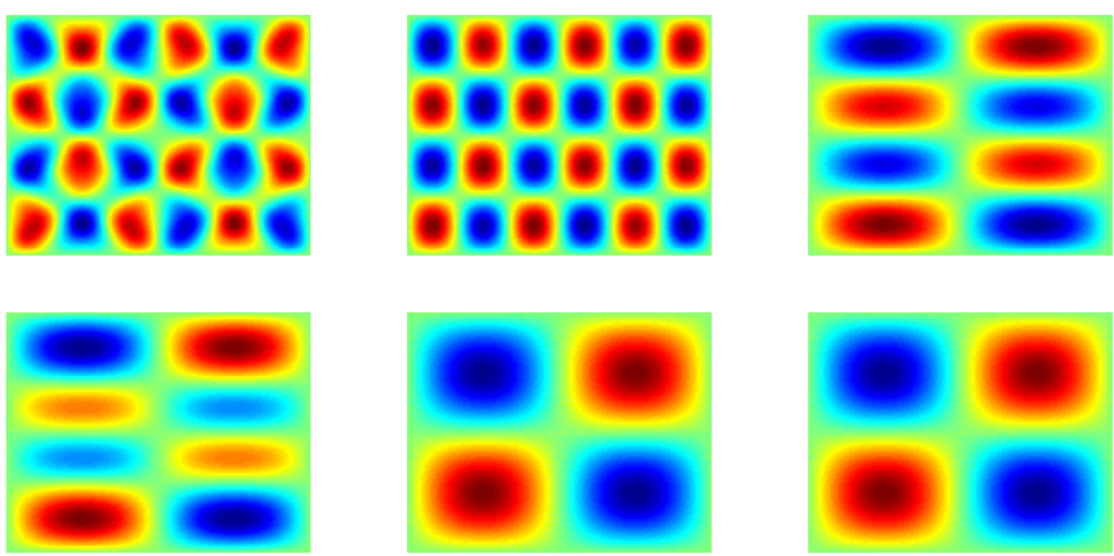

Figure 2 (Color online) The profiles of numerical solutions of the height function ϕ for the MBE equation by using adaptive time strategy at $t = 0, 1, 5, 10, 20, 30$, respectively

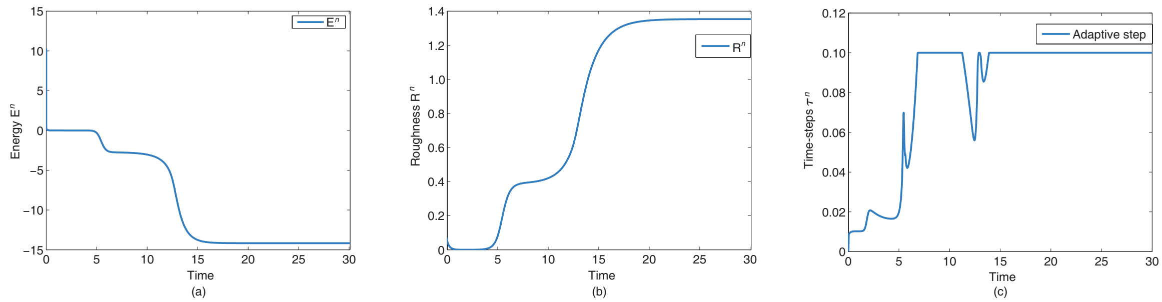

Figure 3 (Color online) Evolutions of energy (a), roughness (b) and adaptive time-steps (c) for the MBE equation by using adaptive time strategy, respectively

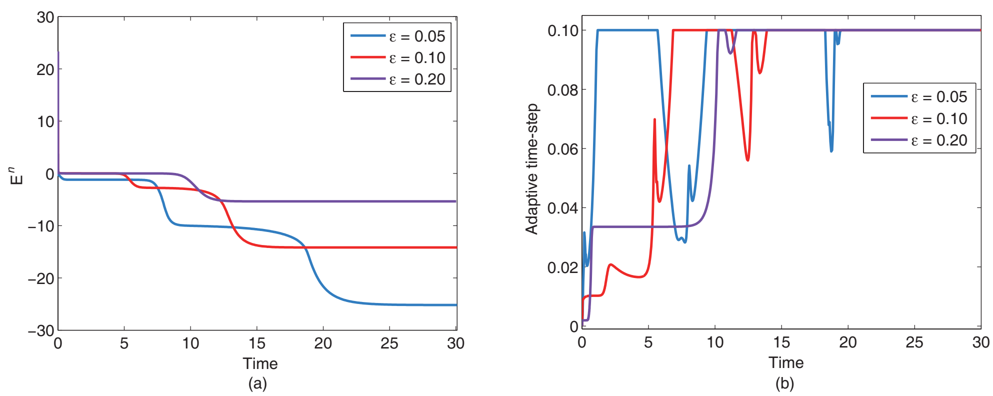

Figure 4 (Color online) Evolutions of energy (a) and time-steps (b) of the MBE equation by using the initial data (5.1) with different $\varepsilon = 0.20$, $\varepsilon = 0.10$ and $\varepsilon = 0.05$ until time $T = 30$

6 Conclusions

We have performed the stability and convergence analysis of the variable-step BDF2 scheme for the molecular beam epitaxial model without slope selection. The main contribution is that we show that the variable-step BDF2 scheme admits an energy dissipation law under the time-step ratio constraint $r_k := \tau_k/\tau_{k-1} < 3.561$. Moreover, the L^2 norm stability and rigorous error estimates are established under the same step-ratio constraint that ensures the energy stability, i.e., $0 < r_k < 3.561$. This is known to be the best result in the literature. We remark that the technique in this work is not applicable to the molecular beam epitaxial model with slope selection, and we shall pursuit this study in our future works.

Acknowledgements The first and second authors were supported by National Natural Science Foundation of China (Grant No. 12071216). The third author was supported by National Natural Science Foundation of China (Grant No. 11731006) and the NNW2018-ZT4A06 project. The fourth author was supported by National Natural Science Foundation of China (Grant Nos. 11822111, 11688101 and 11731006) and the Science Challenge Project (Grant No. TZ2018001). The authors thank the anonymous referees for their valuable comments that are very helpful in improving the quality of this article (arXiv:2008.03185v1).

References

1 Amar J-G, Family F. Effects of crystalline microstructure on epitaxial growth. Phys Rev B, 1996, 54: 14742–14753

2 Becker J. A second order backward difference method with variable steps for a parabolic problem. BIT, 1998, 38: 644-662

3 Chen W, Conde S, Wang C, et al. A linear energy stable scheme for a thin film model without slope selection. J Sci Comput, 2012, 52: 546–562

4 Chen W, Wang C, Wang X. A linear iteration algorithm for a second-order energy stable scheme for a thin film model without slope selection. J Sci Comput, 2014, 59: 574–601

5 Chen W, Wang X, Yang Y, et al. A second order BDF numerical scheme with variable steps for the Cahn-Hilliard equation. SIAM J Numer Anal, 2019, 57: 495–525

6 Cheng Q, Shen J, Yang X-F. Highly efficient and accurate numerical schemes for the epitaxial thin film growth models by using the SAV approach. J Sci Comput, 2019, 78: 1467–1487

7 Crouzeix M, Lisbona F-J. The convergence of variable-stepsize, variable formula, multistep methods. SIAM J Numer Anal, 1984, 21: 512–534

8 Emmrich E. Stability and error of the variable two-step BDF for semilinear parabolic problems. J Appl Math Comput, 2005, 19: 33–55

9 Evans J-W, Thiel P-A. A little chemistry helps the big get bigger. Science, 2010, 330: 599–600

10 Golubovic L. Interfacial coarsening in epitaxial growth models without slope selection. Phys Rev Lett, 1997, 78: 90–93

11 Gomez H, Hughes T. Provably unconditionally stable, second-order time-accurate, mixed variational methods for phase-field models. J Comput Phys, 2011, 230: 5310–5327

12 Gong Y Z, Zhao J, Wang Q. Arbitrarily high-order unconditionally energy stable schemes for thermodynamically consistent gradient flow models. SIAM J Sci Comput, 2020, 42: 135–156

13 Grigorieff R-D. Stability of multistep-methods on variable grids. Numer Math, 1983, 42: 359–377

14 Ju L, Li X, Qiao Z, et al. Energy stability and error estimates of exponential time differencing schemes for the epitaxial growth model without slope selection. Math Comp, 2018, 87: 1859–1885

15 Le Roux M-N. Variable step size multistep methods for parabolic problems. SIAM J Numer Anal, 1982, 19: 725–741

16 Li B, Liu J-G. Thin film epitaxy with or without slope selection. European J Appl Math, 2003, 14: 713–743

17 Liao H-L, Ji B, Zhang L. An adaptive BDF2 implicit time-stepping method for the phase field crystal model. IMA J Numer Anal, 2020, doi:10.1093/imanum/draa075

18 Liao H-L, Tang T, Zhou T. On energy stable, maximum-principle preserving, second order BDF scheme with variable steps for the Allen-Cahn equation. SIAM J Numer Anal, 2020, 58: 2294–2314

19 Liao H-L, Zhang Z. Analysis of adaptive BDF2 scheme for diffusion equations. Math Comp, 2020, doi:10.1090/mcom/3585

20 Qiao Z, Sun Z-Z, Zhang Z. Stability and convergence of second-order schemes for the nonlinear epitaxial growth model without slope selection. Math Comp, 2015, 84: 653–674

21 Qiao Z, Zhang Z, Tang T. An adaptive time-stepping strategy for the molecular beam epitaxy models. SIAM J Sci Comput, 2011, 33: 1395–1414

22 Rost M, Krug J. Coarsening of surface structures in unstable epitaxial growth. Phys Rev E (3), 1997, 55: 3952–3957

23 Shen J, Wang C, Wang X, et al. Second-order convex splitting schemes for gradient flows with Ehrlich-Schwoebel type energy: Application to thin film epitaxy. SIAM J Numer Anal, 2012, 50: 105–125

24 Xu C, Tang T. Stability analysis of large time-stepping methods for epitaxial growth models. SIAM J Numer Anal. 2006, 44: 1759–1779

25 Xu J, Li Y-K, Wu S-N, et al. On the stability and accuracy of partially and fully implicit schemes for phase field modeling. Comput Methods Appl Mech Engrg, 2019, 345: 826–853

26 Yang X-F, Zhao J, Wang Q. Numerical approximations for the molecular beam epitaxial growth model based on the invariant energy quadratization method. J Comput Phys, 2017, 333: 104–127

27 Zhang Z, Ma Y, Qiao Z. An adaptive time-stepping strategy for solving the phase field crystal model. J Comput Phys, 2013, 249: 204–215